Two-dimensional quantum transport in highly conductive carbon nanotube fibers

L. Piraux,* F. Abreu Araujo, and T. N. Bui
Institute of Condensed Matter and Nanosciences, Université catholique de Louvain, Louvain-la-Neuve, Belgium

M. J. Otto
Teijin Aramid, Arnhem, The Netherlands

J.-P. Issi
École Polytechnique de Louvain, Université catholique de Louvain, Louvain-la-Neuve, Belgium
(Received 23 March 2015; revised manuscript received 29 May 2015; published 26 August 2015)

Measurements of the electrical resistivity, from 1.5 to 300 K, and of the low temperature magnetoresistance of highly conductive carbon nanotube (CNT) fibers, obtained by wet-spinning from liquid crystalline phase (LCP), are reported. At high temperature the results obtained on the raw CNT fibers show a typical metallic behavior and the resistivity levels without postdoping process were found to be only one order of magnitude higher than the best electrical conductors, with the specific conductivity (conductivity per unit weight) comparable to that of pure copper. At low temperature a logarithmic dependence of the resistivity and the temperature dependence of the negative magnetoresistance are consistent with a two-dimensional quantum charge transport—weak localization and Coulomb interaction—in the few-walled CNT fibers. The temperature dependence of the phase-breaking scattering rate has also been determined from magnetoresistance measurements. In the temperature range $T <$ 100 K, electron-electron scattering is found to be the dominant source of dephasing in these highly conductive CNT fibers. While quantum effects demonstrate the two-dimensional aspect of conduction in the fibers, the fact that it was found that their resistance is mainly determined by the intrinsic resistivity of the CNTs—and not by intertube resistances—suggests that better practical conductors could be obtained by improving the quality of the CNTs and the fiber morphology.

DOI: 10.1103/PhysRevB.92.085428 PACS number(s): 72.15.Rn, 61.48.De

I. INTRODUCTION

Following the discovery of two-dimensional (2D) quantum interference effects of weak localization (WL) and electron-electron interaction in thin metal films and 2D semiconductor nanostructures [1–4], the same quantum transport phenomena were first observed on a quasi-2D hole gas in bulk carbonaceous materials, intercalated with acceptor species [5,6] and pristine materials [7,8]. Later on, the first measurements performed on individual multiwalled carbon nanotubes (MWNTs) were reported [9]. The results obtained at low temperatures in a MWNT were interpreted in terms of 2D WL, Coulomb interaction, and universal conductance fluctuations. In a previous paper, Song *et al*. [10] observed at low temperature a negative magnetoresistance and an increase in resistivity with decreasing temperature on carbon nanotube bundles, 60 μm diameter, that were also attributed to WL.

Weak localization is a single-particle quantum interference of electron waves resulting in an enhanced back-scattering from multiple elastic scattering events in a diffusive medium. The observation of such an interference effect requires phase-coherent propagation of electron waves. The scattering of electrons by phonons, by the other electrons as well as by paramagnetic impurities are phase-breaking scattering processes which tend to destroy the interference effect responsible for weak localization. The second type of quantum corrections to the electrical conductivity that often coexist with the single-particle interference effect is determined by the interaction between charge carriers in the presence of disorder. Both weak localization and Coulomb interactions are enhanced with increasing disorder, i.e., static defect scattering. Thus, both effects are indicative of the degree of disorder in the sample investigated.

During the last decade, various kinds of carbon nanotube (CNT) assemblies (arrays, films, bundles, etc.) were investigated but, in view of obtaining superior mechanical performance, researchers have focused on CNT fibers. The first CNT fibers were successfully prepared through spinning by Vigolo and co-workers [11]. Well-aligned macroscopic continuous fibers consisting of single-walled (SWNT) or MWNT carbon nanotubes are now produced by conventional spinning (cf. review papers by Behabtu *et al*. [12], Lu *et al*. [13], Lekawa-Raus *et al*. [14], and Sun *et al*. [15]). The fibers combine specific strength, stiffness, and thermal conductivity of carbon fibers with the specific electrical conductivity close to that of metals. The resistivity data reported so far in the literature by other groups working on CNT assemblies obtained by various methods, whether from *LC* phase in sulphuric acid (wet-spinning) or solid (dry-spinning) methods (see, e.g., review papers by Behabtu *et al*. [12] and Lekawa-Raus *et al*. [14]) have shown that the electrical resistivity of these systems is mainly due to intertube resistances, thus not revealing the intrinsic properties of the CNTs.

The air stable, nonintercalated and highly conductive CNT fibers available now [16] should favor the observation of the intrinsic properties of the CNTs and the observation of quantum effects in electrical transport, provided intertube contact resistances are negligible with respect to the CNT resistances at low temperatures. As a corollary, it is expected that the analysis

*Corresponding author: luc.piraux@uclouvain.be

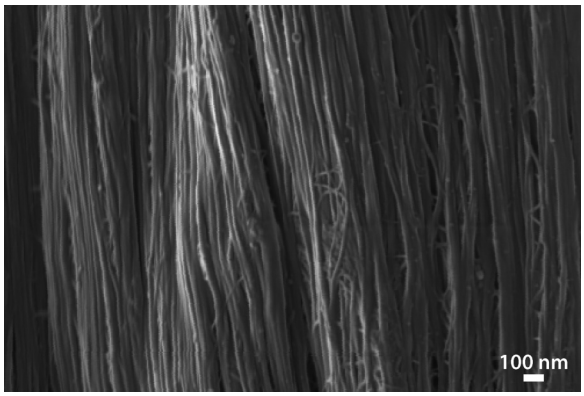

FIG. 1. High resolution SEM picture of CNT fiber spun from chlorosulphonic acid. The morphology consists of highly branched, Y-shape, and very long ropes of densely packed and well-aligned CNTs with diameters in the range 10–100 nm.

of the WL and Coulomb interaction observations should give an indication of the dimensionality of electronic conduction of the CNT fibers.

In the present work we report on the measurement, from 1.5 to 300 K, of the electrical resistivity and magnetoresistance of three samples of such highly conductive raw CNT fibers obtained by means of a wet-spinning method [16]. In these samples, the fiber resistance is found to be mainly determined by the intrinsic resistivity of the CNTs in the entire temperature range. The results at high temperature confirm the metallic behavior, while the low-temperature results are quantitatively interpreted in terms of 2D WL and Coulomb interaction effects.

II. EXPERIMENT

The experimental procedure concerning the preparation and characteristics of the CNT fiber samples are described in more detail elsewhere [16]. Briefly, one can say that few micrometers long CNTs are dispersed homogeneously in chlorosulphonic acid to form a liquid crystalline phase. That LCP dope is then spun by a wet-spinning method, washed and dried to form CNT fibers. In principle the wet spun fibers are of infinite length but for practical reasons, the collected fibers are a few hundred meters long. Different types of CNTs were used to prepare three specific CNT continuous fibers with different features. We labeled them as samples A, B, and C. The raw fiber samples used in the present study consist in predominantly double and single wall (DWNT and SWNT) with only a small amount of MWNTs. In Fig. 1 we present a high resolution scanning electron microscopy (SEM) image of a CNT fiber, showing the Y-branch structure of the CNT ropes.

Electrical transport measurements were performed in a He flow pulse-tube cryocooler with a base temperature of 1.5 K. The electrical resistivity was measured on individual CNT fiber samples between 1.5 and 300 K by means of a classical four-probe dc method. The diameters of the CNT fibers were typically between 11 and 18 μm and the measured samples were about 2 cm long. The electrical contacts were made by gluing a gold wire to the fiber surface with silver paint and the distance between two neighboring contacts ranged from 5 to 10 mm to allow homogeneous current distribution in the fiber samples. For each sample, the input power was kept below 10 μW to avoid self-heating, and the resistance was measured within its Ohmic resistance range with a resolution of one part in 10^5. Magnetic fields up to 6 T were provided by means of a superconducting magnet. The various CNT fiber samples were mounted with the fiber axis perpendicular to the applied magnetic field.

III. RESULTS AND DISCUSSION

In Fig. 2(a), we show the temperature variation of the electrical resistivity, ρ, of the three CNT fiber samples from 1.5 to 300 K. In the higher temperature range, all samples display a metallic behavior, i.e., a decrease in resistivity with decreasing temperature. This metallic behavior and the small values for the room temperature electrical resistivity in the range of 15–55 $\mu\Omega$ cm are reminiscent of doped CNT fibers or intercalated carbon fibers [17] and can be ascribed to sample preparation procedure. Indeed, the as-spun fibers are naturally doped by exposing the CNTs surface to the acid and the residual acid dopant occupies the interstitial spaces between

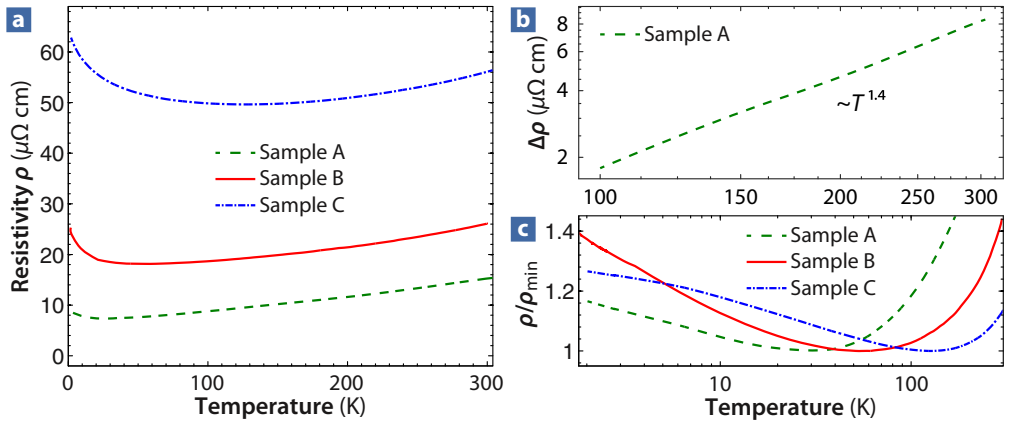

FIG. 2. (Color online) Temperature dependence of the resistivity for the various CNT fiber samples using (a) a linear and (c) a logarithmic temperature scale. For the logarithmic plots, the measured resistance is normalized to the resistivity minimum. In (b), the temperature-dependent resistivity component for sample A is reported in the higher temperature range as a log-log plot.

TABLE I. Sample characteristics and parameters relative to electrical resistivity measurements of the various CNT fibers.

CNT fiber sample	Diameter (μm)	Density (g/cm^3)	$\rho(T = 300$ K) ($\mu\Omega$ cm)	T_{min} (K)
A	16	1.3	15	29
B	18	1.3	26	59
C	11	1.1	56	130

CNTs [16]. Remarkably, this synthesis process allows one to produce raw CNT cables with room temperature electrical resistivity as low as 15 $\mu\Omega$ cm [sample A in Fig. 2(a)], which is to the best of our knowledge the lowest resistivity reported so far for as-spun CNT fibers (i.e., without postdoping or intercalation processes) and is close to the lowest value recorded so far for iodine-doped double-walled CNT fibers [18]. Using the fiber density ($\sim$1.3g/cm^3; see Table I), the specific conductivity (conductivity per unit weight) of sample A, is remarkably large, up to 5.1×10^4S cm^2/g and only slightly less than for pure copper (6.6×10^4 S cm ^{2}/g).

In Fig. 2(b), we present the temperature-dependent component of the resistivity of sample A, the most conductive of the series, in the temperature range 100 K $< T <$ 300 K. We have extracted this component $\Delta\rho(T) = \rho(T) - \rho_0$ from the total measured resistivity, by taking the resistivity in the low-T limit $\rho_0 = 7$ $\mu\Omega$ cm. In the higher temperature range, this temperature-dependent resistivity should be mainly ascribed to electron-phonon interaction. It may be seen that, above 100 K this resistivity varies as $T^{1.4}$. A similar behavior ($T^{1.5}$ variation) was obtained in graphene [19].

For each CNT fiber sample, a minimum of resistivity is found at a given temperature T_{min} below which ρ starts to increase with decreasing temperature. The value of T_{min} depends on the sample and it rises with increasing resistivity value. Similar $\rho(T)$ behavior, including metallic regime in the high T range and low-temperature resistivity minimum, have been recently reported in other highly conductive CNT fibers [16,18]. The low-temperature behavior of resistivity was tentatively interpreted in terms of carrier hopping or tunneling due to inter-CNT transport [16]. However, the hopping mechanism leads to exponential terms for the temperature-dependent electrical resistivity, thus giving rise to a much stronger increase of ρ at low temperature (up to several orders of magnitude over a decade of temperature), as observed in both doped and undoped single-walled CNT fibers [20,21]. In contrast, the increase in resistivity is much smaller for the three samples studied, in the range 10%–30% over one decade of temperature. From the analysis of the results obtained on our samples presented hereafter, it appears that the measured $\rho(T)$ curves on the different fiber samples reflect the intrinsic resistivity of the acid-doped CNTs. The low contact resistance between CNTs can be attributed to synthesizing CNT fibers from liquid crystalline phase and to the branched structure of the CNT ropes (Fig. 1).

As shown in Fig. 2(c), all CNT fibers exhibit a pronounced logarithmic increase of resistivity with decreasing temperature below T_{min}. Since multiwalled carbon nanotubes are essentially two-dimensional electrical conductors [9] and current flow can be described in terms of diffusive charge carrier motion, their transport properties exhibit quantum corrections to the conductivity. Here, we identify two mechanisms to be responsible for the logarithmic anomaly in the $\rho(T)$ curve due to the occurrence of both weak localization and Coulomb interactions in the two-dimensional regime. It should be noted that similar logarithmic dependence effects in $\rho(T)$ were previously observed in acceptor intercalated graphite fibers showing comparable resistance rise and T_{min} values [22,23]. Besides, the log T dependence of ρ for sample C in Fig. 2(c) is followed by a tendency towards resistivity saturation at the lowest temperatures, as already observed in graphite intercalation compounds [22] and multiwalled CNTs [9].

From theoretical considerations [24], it is well known that the observation of negative magnetoresistances in 2D metallic systems constitutes another characteristic feature of the weak-localization phenomenon. In addition, while a relatively weak transverse magnetic field tends to destroy weak localization, it does not influence the resistivity anomaly due to Coulomb interactions. Therefore, the measurement of magnetoresistance at various temperatures can be used to separate the weak-localization contribution from the Coulomb interactions contribution.

For 2D systems without spin-orbit scattering, a uniform perpendicular magnetic field weakens the weak-localization effect when the magnetic field becomes greater than

$$H_\phi = \frac{\hbar}{4eD\tau_\phi}, \tag{1}$$

where τ_ϕ is the relevant phase-breaking scattering time due to electron-phonon scattering, electron-electron scattering, and possibly magnetic scattering; $D = 1/2v_F\ell$ is the diffusion constant; v_F is the Fermi velocity; and ℓ is the elastic mean free path. For magnetic fields smaller than $H = \hbar/(2e\ell^2)$ perpendicular to the 2D electron system and in the absence of spin-orbit scattering, the negative magnetoresistance may be expressed as follows [3,24]:

$$\left[\frac{\Delta R(H)}{R}\right]_{theor} = \frac{R(H) - R(0)}{R(0)} = -\frac{e^2 R_\square}{2\pi^2\hbar}\left[\Psi\left(\frac{1}{2} + \frac{H_\phi}{H}\right) - \ln\left(\frac{H_\phi}{H}\right)\right], \tag{2}$$

where Ψ is the digamma function and $R_\square$ is the resistance per square of the two-dimensional charge carrier gas. In the case $H \gg H_\phi$, the above equation reduces to a simple form:

$$\left[\frac{\Delta R(H)}{R}\right]_{theor} = -\frac{e^2 R_\square}{2\pi^2\hbar}\left[\ln\left(\frac{H}{H_\phi}\right) - 1.9635\right], \tag{3}$$

so that the negative magnetoresistance varies as log H.

Further evidence of 2D localization phenomena in our CNT fibers is manifested through the observation of a negative magnetoresistance over a wide temperature range. The magnetoresistance curves of the different samples are shown in Figs. 3(a)–3(c) as a function of magnetic field at various temperatures, in the range 1.5 K $< T <$ 100 K. It may be seen that the magnetoresistance of all samples is negative and that its magnitude increases with decreasing temperature. The magnetoresistance reaches about 2.5% at $H = 6$ T at the lowest temperature ($T = 1.5$ K) for the more resistive

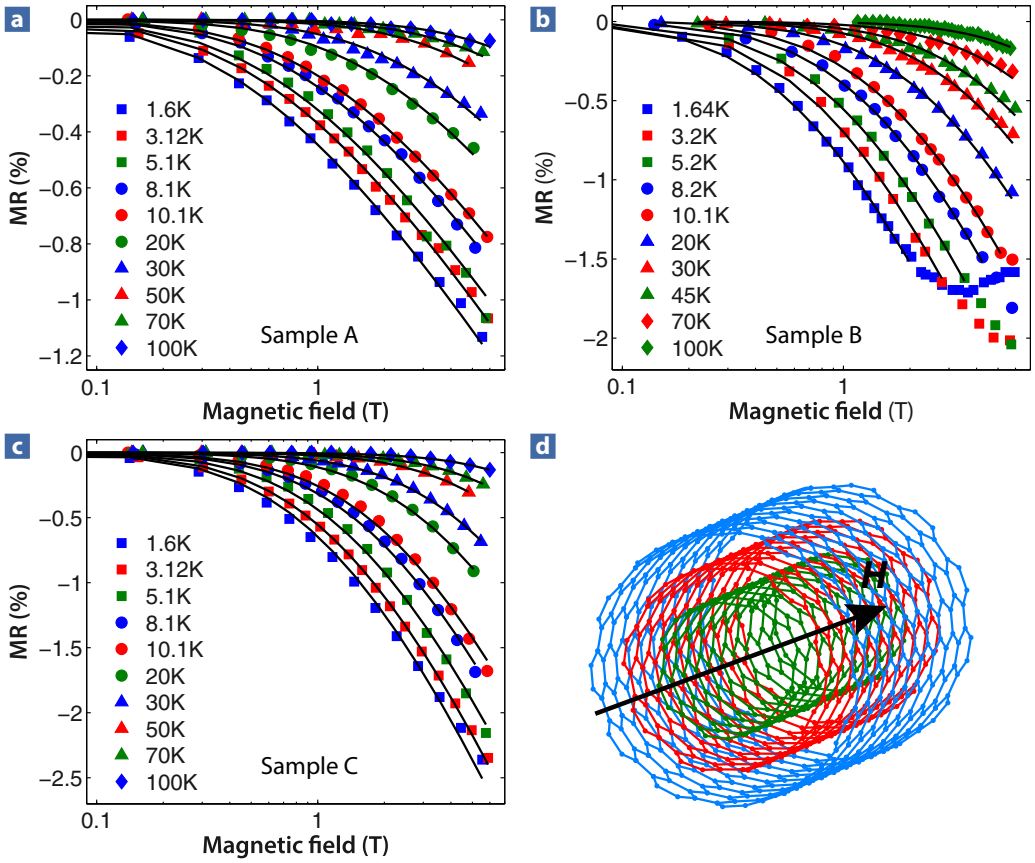

FIG. 3. (Color online) Magnetoresistance vs magnetic field for the various CNT fibers (a) sample A, (b) sample B, and (c) sample C at various temperatures, as indicated. The solid curves are fits to the experimental data using Eqs. (2) and (4). In (d), a schematic drawing of a few-walled CNT is shown. The fitting parameters are summarized in Table I.

sample C, while the magnitude of the effect is reduced by about a factor 2 for the more conductive sample A. In the high field range, a log H variation of the magnetoresistance is observed for all CNT fiber samples, which is consistent with Eq. (3). In addition, the log H behavior appears at higher fields as the temperature increases, as expected from the enhancement of H_ϕ with temperature.

Now let us concentrate on the magnetoresistance results reported in Figs. 3(a)–3(c) that we assume to be only due to 2D weak localization. Since our CNT fibers consist of a few concentric tubes of graphene [see Fig. 3(d)], and that only the component of the field perpendicular to the graphene layers acts to destroy the weak-localization contribution, our experimental curves were fitted to the following expression [23]:

$$\left[\frac{\Delta R(H)}{R}\right] = \frac{1}{\pi}\int_{-\pi/2}^{\pi/2}\left[\frac{\Delta R(H\cos\theta)}{R}\right]_{\text{theor}} d\theta, \qquad (4)$$

where θ is the angle between the normal to a graphene layer and the magnetic field direction. We thus average the magnetoresistance over all possible angles θ between the applied magnetic field and the graphene planes. In this analysis, the much smaller parallel magnetoresistance is neglected.

The solid lines of Figs. 3(a)–3(c) correspond to the best fit of the predictions of Eqs. (2) and (4) to the experimental data using $R_\square$ and H_ϕ as fitting parameters. $R_\square$ is assumed to be independent of temperature, while H_ϕ was allowed to vary independently at each temperature. We see that the fits reproduce quite well the experimental results. The parameters obtained from the fit are given in Table II for all CNT fibers.

A plot of H_ϕ as a function of T is shown in Fig. 4. For each of the CNT fiber samples, H_ϕ [and consequently the phase-breaking rate $1/\tau_\phi$, from Eq. (1)] exhibits an approximately linear temperature dependence except in the lowest temperature range. Such behavior can be qualitatively understood in terms of the current theory for electron-electron scattering in 2D disordered systems [25]. Using Eq. (1), the characteristic length scale $L_\phi = \sqrt{D\tau_\phi}$ over which a charge carrier loses the coherence of its wave function due to electron-electron scattering is numerically determined by the

TABLE II. Parameters describing the weak-localization effect in CNT fibers; $R_\square$ and H_ϕ/T are obtained from the fit of the magnetoresistance results using Eqs. (2) and (4); L_ϕ is calculated using Eq. (1) and H_ϕ value at $T = 20$ K.

CNT fiber sample	$R_\square$ ($\Omega/\square$)	H_ϕ/T (10^{-2} T/K)	L_ϕ (20 K) (nm)
A	440	1.5	25
B	1325	2.0	20
C	1513	2.6	17

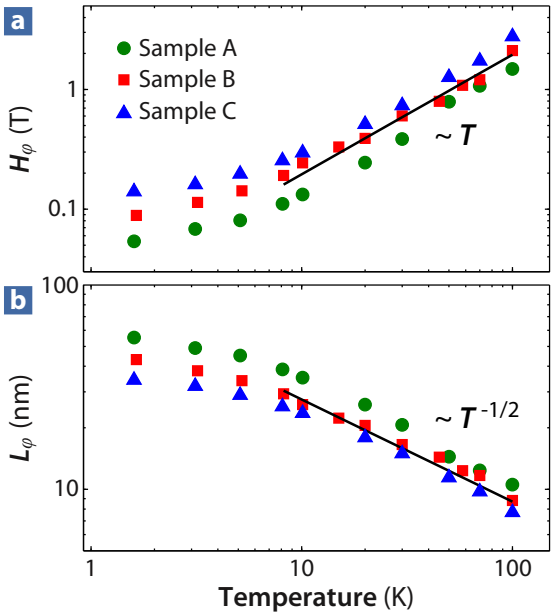

FIG. 4. (Color online) Temperature variation of the characteristic magnetic field H_ϕ and length scale L_ϕ for phase-breaking scattering mechanisms for each CNT fiber sample.

expression $L_\phi = \sqrt{h/(4eH_\phi)}$ and is also reported in Fig. 4. As may be seen, L_ϕ varies as $T^{-1/2}$ for all CNT fiber samples in the range 10 K $< T <$ 100 K. The same temperature dependence for L_ϕ below 10 K was found in a previous work performed on undoped individual multiwalled CNTs [9].

Now let us consider the phase-breaking mechanism, which is found to predominantly arise from the influence of carrier-carrier scattering. According to Altshuler *et al.* [25], the electron-electron scattering rate for 2D disordered systems in the case of quasielastic collisions may be written as

$$\frac{1}{\tau_{e\text{-}e}} = kT\frac{e^2R_\square}{2\pi\hbar^2}\ln\left(\frac{\pi\hbar}{e^2R_\square}\right). \quad (5)$$

It should be mentioned that evidence for such electron-electron scattering with small energy transfers has been found in most of the weakly disordered 2D electron systems studied so far for temperatures less than 10 K, while inelastic electron-phonon scattering dominates at higher temperatures [26]. In the present study on CNT fibers, the observed linear T dependence of $1/\tau_\phi$ even extends up to 100 K.

We now compare the experimentally deduced carrier-carrier phase-breaking scattering rate for a given sample with the theoretical predictions of Eq. (5). For the case of sample B, using a rough estimate of the diffusion constant $D \sim 10^{-3}$ m^2/s [27] and the value of the linear coefficient for $H_\phi(T)$ given in Table II, we obtain from Eq. (1), $1/\tau_\phi = 1.2 \times 10^{11}$ T/s. On the other hand, Eq. (5) predicts for the same sample $1/\tau_{e\text{-}e} = 3.1 \times 10^{10}$ T/s. For the CNT fiber samples considered in the present study, the values of $\tau_{e\text{-}e}$ calculated from Eq. (5) differ from the experimental values of τ_ϕ by about a factor 4 to 5, but such a disagreement is acceptable in view of the estimates used for the diffusion constant D.

Alternately, the predictions for electron dephasing due to inelastic e-e scattering in 2D dirty metals lead to a slightly modified $T\ln T$ form for $1/\tau_{e\text{-}e}$ [28].

$$\frac{1}{\tau_{e\text{-}e}} = \frac{kT}{2\varepsilon_F\tau}\ln\left(\frac{4(\varepsilon_F\tau)^2D\kappa^2}{\hbar kT}\right), \quad (6)$$

where ε_F is the Fermi energy, τ is the elastic scattering time, and κ is the effective inverse screening length. The uncertainty associated with several parameters in Eq. (6) for our CNT fibers lead to unreliable estimates of the scattering rate $1/\tau_{e\text{-}e}$.

Furthermore, one cannot reliably distinguish between the T and $T\ln T$ temperature dependencies over this range of temperature taking into account the experimental uncertainty in the determination of $1/\tau_\phi$. However, the observation of a linear or quasilinear temperature dependence of the phase-breaking rate clearly indicates that electron-electron scattering constitutes the dominant phase-breaking mechanism in such few-walled CNT fibers below 100 K.

For sample B, we also observed the onset of a positive contribution to the magnetoresistance below $T = 3$ K for $H > 2$ T [see Fig. 3(b)]. A similar positive upturn of magnetoresistance at low temperature was previously reported on other CNT systems [29], although its physical interpretation is still under debate.

In addition, in the lowest temperature range investigated, H_ϕ shows a tendency to reach a saturated value for all CNT fiber samples (see Fig. 4). Such saturation of the dephasing time can be due to an extrinsic mechanism caused by magnetic scattering [3] and has been revealed in previous results obtained on graphite intercalation compounds [22] and multiwalled CNTs [9]. Although the microscopic origin of magnetic scattering is still unknown, it can be due to some residual magnetic impurities coming from the transition metal catalysts used in the synthesis of the CNTs.

In Fig. 5, we illustrate the effect of a magnetic field on the rate of the logarithmic increase of resistance, by superimposing the experimental results for sample A and the calculated

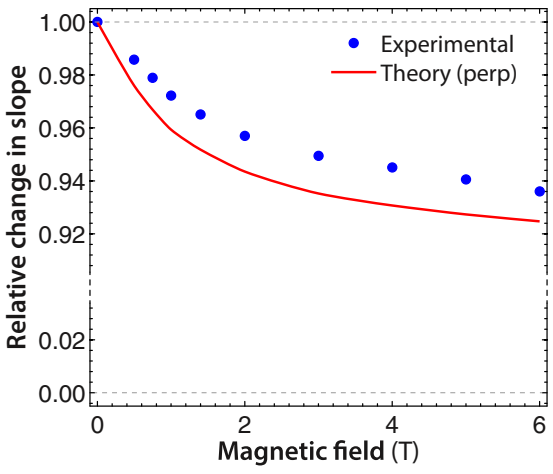

FIG. 5. (Color online) Relative differences in slope of the logarithmic temperature dependence of the resistivity with magnetic field for sample A ($\Delta R/R_{\text{decade}} \sim 13\%$ at zero field). The blue dots are the experimental points obtained at various transverse magnetic fields to the fiber axis. The continuous red line is the numerical calculations using Eq. (2) for a fully perpendicular magnetic field to the graphene layers.

values using Eq. (2) that would be observed if the magnetic field was fully perpendicular to the graphene layer. Even if no complete saturation is reached at the maximum field of 6 T, we may anticipate that the magnetic field introduces only a small reduction to the coefficient of the logarithmic variation. A similar behavior was found on the different CNT fiber samples. So, while the analysis of magnetoresistance results provides evidence for 2D weak localization, it can be concluded that the logarithmic dependence of the resistivity is predominantly due to the Coulomb interactions effect. To corroborate the result, anomalies in the low-temperature dependence of the thermoelectric power in multiwalled CNTs have been explained by considering the effects of Coulomb interaction in the presence of defect scattering in weakly disordered electron systems [30].

IV. CONCLUSION

In the present work, we have measured the electrical resistivity from 1.5 to 300 K and the low-temperature magnetoresistance of three samples of highly conductive CNT fibers obtained by wet-spinning without postdoping process.

In the higher temperature range, the results show a typical metallic behavior: the resistivity increases with increasing temperature due to electron-phonon interaction. In the lower temperature region, all the experimental features observed, i.e., the logarithmic anomaly in the ρ curve and the shape and temperature dependence of the negative magnetoresistance are consistent with a two-dimensional charge transport in such few-walled CNT fibers. The temperature dependence of the phase-breaking scattering rate has also been determined from magnetoresistance measurements. In the temperature range $T < 100$ K, electron-electron scattering is found to be the dominant source of dephasing in these highly conductive CNT fibers. The temperature dependence of the CNT fiber resistivity and the consistent picture for the magnetoresistance behavior indicates that the electrical transport properties of the CNT fibers are mainly determined by the intrinsic feature of the carbon nanotubes.

In addition, it may be seen that, together with the knowledge of the resistivity value, the interpretation of the low-temperature results provides a tool for characterization of the CNT fibers investigated. On the one hand, the analysis of the quantum effects observed confirms the two-dimensional aspect of electronic conduction in the system. On the other hand, the resistivity levels confirm the high structural perfection of the raw fiber material as ρ can be as low as 15 $\mu\Omega$ cm, so only by a factor 10 higher than the best electrical conductors. The specific conductivity (conductivity per unit weight) of sample A, is remarkably large, and only 20% less than for pure copper. Our results show great potential for the development of practical electrical conductors with better electrical and physical properties than pure metals via further optimization of the fiber and constituting ropes morphology and by using CNTs of higher conductivities.

ACKNOWLEDGMENTS

We are grateful to Ron Ter Waarbeek and Dr. Jorrit de Jong for spinning CNT fibers and to Ed Steyn for taking HR SEM pictures. We acknowledge funding their work by Teijin Aramid BV and Teijin Ltd. This work was partly supported by the Fédération Wallonie-Bruxelles (ARC 13/18-052 Supracryst). Finally, F.A.A. acknowledges the UCL for an FSR complement (Fonds Spécial de Recherche).

[1] E. Abrahams, P. W. Anderson, D. C. Licciardello, and T. V. Ramakrishnan, Scaling Theory of Localization: Absence of Quantum Diffusion in Two Dimensions, Phys. Rev. Lett. **42**, 673 (1979).

[2] B. L. Altshuler and A. G. Aronov, Zero bias anomaly in tunnel resistance and electron-electron interaction, Solid State Commun. **30**, 115 (1979).

[3] G. Bergmann, Weak localization in thin films: A time of-flight experiment with conduction electrons, Phys. Rep. **107**, 1 (1984).

[4] B. L. Altshuler and A. G. Aronov, Electron-electron interaction in disordered conductors, in *Electron–Electron Interactions in Disordered Systems*, edited by A. Efros and M. Pollak, Modern Problems in Condensed Matter Sciences Vol. 10 (Elsevier, New York, 1985), pp. 1–153.

[5] L. Piraux, J.-P. Issi, J.-P. Michenaud, E. McRae, and J. F. Marêché, Evidence for hole localization in a low stage acceptor graphite intercalation compound, Solid State Commun. **56**, 567 (1985).

[6] L. Piraux, V. Bayot, X. Gonze, J. P. Michenaud, and J. P. Issi, Effect of a magnetic field on weak localization and Coulomb interactions in acceptor graphite intercalation compounds, Phys. Rev. B **36**, 9045 (1987).

[7] V. Bayot, L. Piraux, J.-P. Michenaud, and J.-P. Issi, Weak localization in pregraphitic carbon fibers, Phys. Rev. B **40**, 3514 (1989).

[8] V. Bayot, L. Piraux, J.-P. Michenaud, J.-P. Issi, M. Lelaurain, and A. Moore, Two-dimensional weak localization in partially graphitic carbons, Phys. Rev. B **41**, 11770 (1990).

[9] L. Langer, V. Bayot, E. Grivei, J.-P. Issi, J. P. Heremans, C. H. Olk, L. Stockman, C. Van Haesendonck, and Y. Bruynseraede, Quantum transport in a multiwalled carbon nanotube, Phys. Rev. Lett. **76**, 479 (1996).

[10] S. N. Song, X. K. Wang, R. P. H. Chang, and J. B. Ketterson, Electronic properties of graphite nanotubules from galvanomagnetic effects, Phys. Rev. Lett. **72**, 697 (1994).

[11] B. Vigolo, A. Pénicaud, C. Coulon, C. Sauder, R. Pailler, C. Journet, P. Bernier, and P. Poulin, Macroscopic Fibers and Ribbons of Oriented Carbon Nanotubes, Science **290**, 1331 (2000).

[12] N. Behabtu, M. J. Green, and M. Pasquali, Carbon nanotube-based neat fibers, Nano Today **3**, 24 (2008).

[13] W. Lu, M. Zu, J.-H. Byun, B.-S. Kim, and T.-W. Chou, State of the art of carbon nanotube fibers: Opportunities and challenges, Adv. Mater. **24**, 1805 (2012).

[14] A. Lekawa-Raus, J. Patmore, L. Kurzepa, J. Bulmer, and K. Koziol, Electrical properties of carbon nanotube based fibers

and their future use in electrical wiring, Adv. Funct. Mater. **24**, 3661 (2014).

[15] G. Sun, Y. Zhang, and L. Zheng, Fabrication of microscale carbon nanotube fibers, J. Nanomaterials **2012**, 506209 (2012).

[16] N. Behabtu, C. C. Young, D. E. Tsentalovich, O. Kleinerman, X. Wang, A. W. K. Ma, E. A. Bengio, R. F. ter Waarbeek, J. J. de Jong, R. E. Hoogerwerf, S. B. Fairchild, J. B. Ferguson, B. Maruyama, J. Kono, Y. Talmon, Y. Cohen, M. J. Otto, and M. Pasquali, Strong, light, multifunctional fibers of carbon nanotubes with ultrahigh conductivity, Science **339**, 182 (2013).

[17] T. C. Chieu, M. S. Dresselhaus, and M. Endo, Raman studies of benzene-derived graphite fibers, Phys. Rev. B **26**, 5867 (1982).

[18] Y. Zhao, J. Wei, R. Vajtai, P. M. Ajayan, and E. V. Barrera, Iodine doped carbon nanotube cables exceeding specific electrical conductivity of metals, Sci. Rep. **1**, 1 (2011).

[19] D. K. Efetov and P. Kim, Controlling Electron-Phonon Interactions in Graphene at Ultrahigh Carrier Densities, Phys. Rev. Lett. **105**, 256805 (2010).

[20] M. Salvato, M. Lucci, I. Ottaviani, M. Cirillo, S. Orlanducci, E. Tamburri, V. Guglielmotti, F. Toschi, M. L. Terranova, and M. Pasquali, Low temperature conductivity of carbon nanotube aggregates, J. Phys.: Condens. Matter **23**, 475302 (2011).

[21] M. Salvato, M. Lucci, I. Ottaviani, M. Cirillo, E. Tamburri, I. Cianchetta, V. Guglielmotti, S. Orlanducci, M. L. Terranova, and M. Pasquali, Effect of potassium doping on electrical properties of carbon nanotube fibers, Phys. Rev. B **84**, 233406 (2011).

[22] L. Piraux, Weak localization and coulomb interaction in graphite intercalation compounds and related materials, J. Mater. Res. **5**, 1285 (1990).

[23] L. Piraux, V. Bayot, J. P. Issi, M. S. Dresselhaus, M. Endo, and T. Nakajima, Influence of magnetic fields on the two-dimensional electron transport in weakly disordered fluorine-intercalated graphite fibers, Phys. Rev. B **45**, 14315 (1992).

[24] S. Hikami, A. I. Larkin, and Y. Nagaoka, Spin-orbit interaction and magnetoresistance in the two dimensional random system, Prog. Theor. Phys. **63**, 707 (1980).

[25] B. L. Altshuler, A. G. Aronov, and D. E. Khmelnitsky, Effects of electron-electron collisions with small energy transfers on quantum localisation, J. Phys. C **15**, 7367 (1982).

[26] J. J. Lin and J. P. Bird, Recent experimental studies of electron dephasing in metal and semiconductor mesoscopic structures, J. Phys.: Condens. Matter **14**, R501 (2002).

[27] T. Tsuneta, L. Lechner, and P. J. Hakonen, Gate-controlled Superconductivity in a Diffusive Multiwalled Carbon Nanotube, Phys. Rev. Lett. **98**, 087002 (2007).

[28] E. Abrahams, P. W. Anderson, P. A. Lee, and T. V. Ramakrishnan, Quasiparticle lifetime in disordered twodimensional metals, Phys. Rev. B **24**, 6783 (1981).

[29] G. T. Kim, E. S. Choi, D. C. Kim, D. S. Suh, Y. W. Park, K. Liu, G. Duesberg, and S. Roth, Magnetoresistance of an entangled single-wall carbon-nanotube network, Phys. Rev. B **58**, 16064 (1998).

[30] N. Kang, L. Lu, W. J. Kong, J. S. Hu, W. Yi, Y. P. Wang, D. L. Zhang, Z. W. Pan, and S. S. Xie, Observation of a logarithmic temperature dependence of thermoelectric power in multiwall carbon nanotubes, Phys. Rev. B **67**, 033404 (2003).